# Comparative Analysis of Discrete Time Simulations and Stochastic Geometry Models of a Single Gateway LoRaWAN Network

Bruno Citoni, Shuja Ansari, Qammer Hussain Abbasi, Muhammad Ali Imran, Sajjad Hussain
*School of Engineering*
*University of Glasgow*
Glasgow, Scotland
b.citoni.1@research.gla.ac.uk

***Abstract*—Both stochastic geometry and discrete-time simulations are useful ways to analyse otherwise unfeasible large-scale LoRaWAN networks. Currently, very limited research has been performed on assessing how the two methods compare in terms of their results when modelling the same scenario. In this study, such a comparison is performed by replicating via discrete time simulations performed with NS-3 a common result from stochastic analysis of a single gateway network. Results of the comparison show how the two methods are for the most part equivalent and thus they are both equally employable in future research. However, attention needs to be paid to the subtle differences that are characteristic of the two different methods and can give rise to discrepancies in results.**

***Index Terms*—IoT, LoRaWAN, NS3, Stochastic geometry**

## I. Introduction

The Internet of Things (IoT) has been hailed as a revolutionary technology that will have an impact on a plethora of activities by monitoring, controlling and reacting to data using an internet-connected network of devices.

The applications of such technology span over multiple industries, such as the agricultural [1], automotive [2] and oil and gas [3]. Furthermore it finds applications in smart city and smart home scenarios, from monitoring the occupancy of parking lots or seats in a library, to scheduling street lights dynamically based on traffic, or providing feedback about the fullness of refuse bins, all the way to personal health monitoring. While these application have different inputs and outputs and some key differences, they all share the need for an underlining communication technology capable of supporting a massive concurrent number of connected devices that can communicate over great distances and using as little energy as possible [4], [5].

Established long-range protocols like satellite and cellular or short-range ones such as Wi-Fi and Bluetooth are not entirely suitable for IoT deployments. Long-range ones have too high energy consumption for devices that are meant to be operated with batteries and deployed in rural or hard to access regions, with minimal maintenance required. Shorter range protocols on the other hand, while being less taxing on a device battery also do not have enough coverage to be fit for most IoT applications.

One protocol that gathered traction in recent years is LoRaWAN: a LPWAN (Low Power Wide Area Network) protocol which satisfies the fundamental IoT requirements. Out of various LPWAN that have been proposed in recent years, LoRaWAN has been regarded as the best protocol for IoT due to its range, power consumption and capital costs.

Because of the nature and the relative youth of the technology, very large scale networks have not yet been implemented in real life. Theoretically, the limits of this technology have been extensively studied, especially those concerning its scalability [6]. To help analyse these specific scenarios, both stochastic geometry and discrete-time simulations are invaluable tools [7]–[9], as they do not require a real network with thousands of devices to be physically implemented. As both approaches are utilised in literature in different scenarios, it is important to establish that the results stemming from the two different analysis methods are comparable so that they can used interchangeably depending on the ease of application in the specific context.

Such a novel comparison is performed in this work by recreating results originally obtained by stochastic models with discrete time simulations performed with the NS-3 simulator.

The rest of this paper is structured as follows. In Sec. II we give a brief overview of the LoRaWAN technology and its limits regarding scalability. In Sec. III we analyse relevant literature and in Sec. IV we introduce our NS-3 simulation setup aimed at recreating a common result from stochastic geometry models. The results of this comparison are then discussed in Sec. V, before concluding remarks are given in Sec. VI.

## II. LoRaWAN technology

LoRaWAN is a protocol built upon the LoRa (Long Range) modulation technique and operates on the licence-free ISM (Industrial, Scientific and Medical) frequencies: 863-870 MHz for the EU region [10].

The regulations on these frequencies limit the duty cycle to 1%, meaning a device can only transmit 1% of the time, before remaining "silent" for a time proportional to the ToA

of the latest packet and the duty cycle enforced according to the following:

$$T_{silence} = T_{air}(\frac{1}{dc} - 1), \quad (1)$$

where

- $T_{silence}$ = Time-of-Silence required after transmission
- $T_{air}$ = Time-on-Air (ToA) of a packet
- $dc$ = duty cycle.

This restricts the maximum airtime per device to about 36 seconds per day. The gateways need to respect this same duty cycle when transmitting, which means this technology is focused much more on uplink than downlink. This limitation makes LoRaWAN unsuitable for high data rate, time-critical, low-latency applications.

### A. Scalability limits

One of the most important metrics that characterise the quality of a network is its Packet Delivery Ratio (PDR). This is an indication of the percentage of data that is successfully transmitted and successfully decoded by any gateway in range and is defined as:

$$PDR = 100 \times \frac{packetsReceived}{packetsSent} \quad (2)$$

This is directly correlated with the data rate of each node and the Time-On-Air (ToA) of a packet. In turn, the ToA is mostly influenced by the Spreading Factor (SF) of the transmission, a LoRa parameter related to the number of chirps that are used to modulate the signal, which can be varied from 7 to 12.

Lower SFs transmissions achieve a higher data rate and have a much shorter ToA, but have also a shorter range as they need to reach the receiver with a higher signal power to be correctly decoded. Higher SFs achieve significantly longer coverage by decreasing the threshold for successful decoding but at the cost of an exponentially longer transmission time and greater power consumption.

A packet must also survive the interference from external sources and concurrent packets sent on the same frequency and SF (and to a lesser extent different SF as well [11]). Because of what is defined as the capture effect, if a packet reaches the receiving gateway with a certain power difference with respect to the stronger interferer than it can still be successfully decoded, otherwise it is lost. The chance of destructive interference between packets depends on the nodes density, their location and their SF, the packet transmission delay and the packet ToA.

Another reason for packet loss is the lack of available receiver's demodulation paths. Successfully receiving a packet involves at first a gateway "locking on" a packet preamble using one of the possible demodulating paths before checking that the SNR (signal-to-noise) and SIR (signal-to-interference ratio) levels are high enough for it to be properly decoded. This process occupies one of the demodulating paths of the gateway for an amount of time proportional to the ToA of the packet. If all the available paths of a gateway are occupied, the next packet arriving will not be received. The probability of saturating a receiver's paths depends on the packets ToA, the nodes density and location, the transmission delay between packets and the capacity of the gateways, which is usually 8 channels for commercially available ones.

Finally, as mentioned in Eq. 1 each device has to adhere to the 1% duty cycle limitation at all times, remaining "silent" for a time proportional to the ToA of the latest packet sent on each sub-band. As the transmission delay is setup by the network designer to be above this value, this is often overlooked as a possible cause of packet loss. However, there may be cases, such as with the use of an adaptive duty cycle algorithm, where the SF a node transmits with changes, affecting the ToA of subsequent transmissions. If this ends up being faster than the Time-of-Silence imposed by the regulations, it would result in "invisible" packet loss. The transmission would formally not happen, hence the packet is technically never lost, but if that data point is not queued up for later transmission then the device will simply discard it, before reading and sending a new data point when next allowed. This loss would not appear in the PDR calculation using eq. (2), and for this reason is vital that this loss cause is kept in mind by the network's designer.

It is important to note how all these conditions need to be true at all times as even a single one failing will make cause a packet to be lost.

## III. Relevant literature

Because of the complexity and the practical issues surrounding the deployment of a large-scale network, the pursuit of a generalised network model to study such scenarios has been a popular avenue in LoRaWAN research. The work done by Georgiou et. al. in [7] is among the firsts to use stochastic geometry to model the behaviour of a LoRaWAN network. Here the authors present a model for a single gateway network, with nodes distributed around it uniformly. The model assumes perfect orthogonality between different SFs, thus ignoring the impact of inter-SF interference. It also neglects the effects of having a limited number of demodulator paths on the overall outage probability and models uplink traffic only. The same scenario with the same limitations is built upon to include non-uniform nodes distributions in [12] as well as a second gateway in [13].

The setup performed in [14] is similar, with a single central gateway, though this work incorporates the effect of quasi-orthogonality of the spreading factors, using an updated collision matrix calculated by [11]. Once again the practical limitation of having a finite number of parallel demodulation paths at the receiver is ignored and so is downlink traffic. One of the few studies to take this limit into account is the one performed in [15]. This paper analyses a single gateway network with 8 parallel demodulation paths, while limiting the complexity in other ways, such as assuming perfect orthogonality.

In most cases, because of the layers of complexity of a rigorously accurate scenario, papers dealing with stochastic models of LoRaWAN networks limit the scope of the analysis

to simplified albeit less realistic configurations. This is usually done by reducing the number of variables present in the network itself.

On the other hand, discrete time simulations are more easily set up, requiring no knowledge of stochastic geometry and performed using existing libraries and software, although they lack the flexibility to "zoom in" and isolate each moving part of the LoRaWAN behaviour.

A popular simulator is LoRaSIM, developed in [16] by Bor et. al. with insight from their experimental results. Among the papers using this simulator are [17], [18] and the research performed by Cuomo et. al. in [8], [19], [20]. This is carried out using a modified version of the LoRaSIM simulator and is focused on the characterisation of different algorithms to allocate SFs in a network to increase the overall quality of service. The simulator works well in this scenario as all that is required to perform the characterisation is the PDR of the network and not more granular variables, such as the effect of each loss on the same PDR.

Another popular way to perform discrete-time simulations of networks is using NS-3, a network simulator built in C++. [21] and [9] were among the first published works to use this simulator, with the development of LoRaWAN specific modules to be integrated with the existing simulator core. Both authors focused on scalability analysis and the release of the code developed by Magrin et. al. in [9] allowed others to modify the LoRaWAN specific modules and reuse them. Other than studying scalability, NS-3 has been used extensively ever since to perform all kind of analysis regarding LoRaWAN, from comparison with other protocols [22] to energy consumption assessments [23].

While both techniques have been used in literature to provide answers regarding the performance of LoRaWAN, they have rarely been compared and used together, with the only attempt found in a preprint paper by Magrin et.al. [24]. In this study, the authors use stochastic geometry to first model a single gateway network, including all known cases of packet loss and both uplink and downlink. Then they validate the results using a modified version of their own LoRaWAN modules for NS-3.

## IV. NS-3 Simulation Setup

The LoRaWAN modules for NS-3 developed in [9] went through additional changes to replicate at the best of our possibilities the assumptions and setup of the stochastic analysis performed in [12]. As mentioned in Section III, stochastic models usually "downgrade" some aspects of LoRaWAN's behaviour to keep the complexity of the mathematical analysis low. Some of these downgrades performed in [12] in respect to a realistic scenario are:

- The use of a single frequency channel at 868.1MHz in contrast to the mandatory three default channels for LoRaWAN in EU (868.1, 868.3 and 868.5MHz), or the eight used by commercially available hardware (868.1, 868.3 and 868.5, 867.1, 867.3, 867.5, 867.7, 867.9MHz)
- The lack of a limit to the amount of packets that can be received concurrently due to the available number of parallel demodulators on commercially available gateways.
- The use of a custom rejection matrix to deal with interference that specifies a 1dB power difference for the capture effect to occur and also assumes perfect orthogonality between different SFs.

The number of nodes in the simulation is set to the average result of the Poisson Point Process (PPP) using the intensity of 3 devices per km$^2$ described and are positioned uniformly within a radius of 10755 meters. The SFs for the nodes are assigned following the common method of simply using the lowest possible SF per node that will give a strong enough link to survive the drop in power caused by the path loss. The standard Friis propagation model implemented in NS-3 was also slightly modified to match that described. This allowed the boundaries between SFs to be consistent (3259, 4209, 5436, 7021, 8690 and 10755 meters), and together with the SF allocation policy gave rise to the network topology shown in Fig. 1.

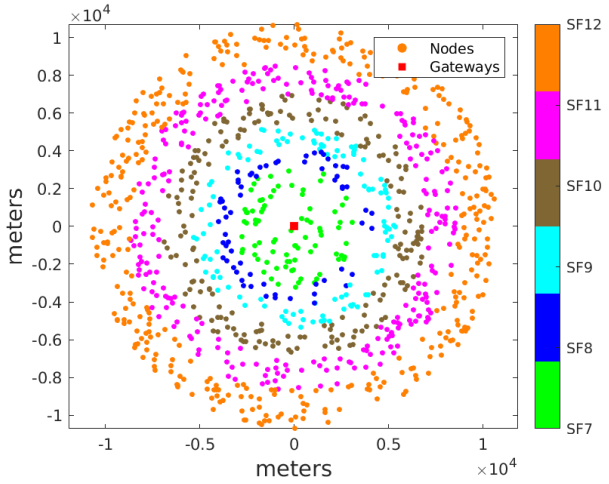


Fig. 1: Network topology featuring a single, central gateway and uniformly distributed nodes with SF allocation based on their distance to the gateway

Due to the nature of the discrete time simulator, or the complexity of matching them by modifying the underlining core functionality of NS-3, the specific, shorter packets ToA and the random time delay between packets illustrated in Section III of [12] were not implemented in this work. Instead, each node transmits 12 bytes of payload (plus 13 of necessary header for LoRaWAN) at a fixed speed that is dependent on the node's SF and the ToA of each packet. Each node hence transmits as often as it can while remaining under the duty cycle limitation of 1%. This gives transmission delays of 6.138, 11.286, 20.394, 40.788, 81.576 and 146.817 seconds for SFs from 7 to 12, respectively.

## V. Results & Analysis

The particular result that was recreated is the peculiar shape of graph of the probability of packet loss as a function of the distance of nodes to a single, central gateway. This result is found in a number of papers such as [12], [7] and [14].

While the details and setups of the models in these works are not the same, the resulting graphs are comparable. The calculated, theoretical PDR (or the probability that a packet survives all outage conditions) has in all cases a distinctive "sawtooth" shape, as shown in Fig. 2.

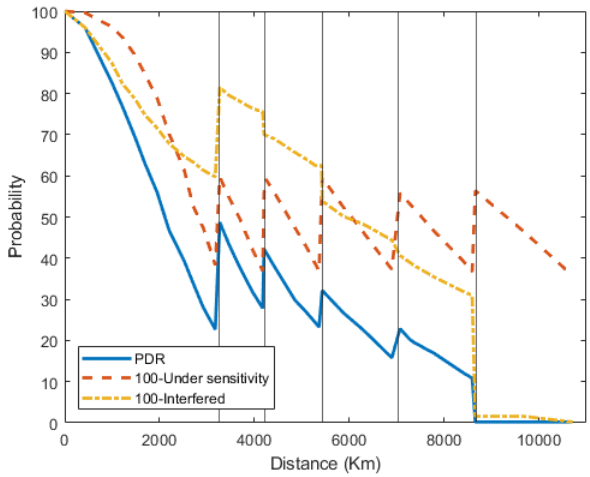


Fig. 2: The success probability of a packet against the distance from a gateway of the node sending it, reproduced from [12]. In blue the overall success probability, in orange the complementary to the probability of collision and in red the complementary to the probability of the packet being under sensitivity

Visual analysis of this result raises a few important points. As expected, the overall probability of a packet being received and decoded correctly drops considerably the further from a gateway the transmitting node is. The distinctive "sawtooth" shape of the red and blue curves in Fig. 2, which are the probability that a packet survives the under sensitivity outage condition and the overall success probability of a packet respectively, is due to the fact that once a certain distance is reached the nodes switch to the next SF, thus lowering the threshold in receive power that the gateway needs to decode their packets correctly. The increase in both probabilities happens at the edge between SF boundaries.

As a first step these results were recreated using the discrete time simulation offered by NS-3, after matching inputs to the best of possibilities as per described in Section IV.

While the under sensitivity and the PDR curves look satisfactory, given the inherently different methods used to recreate them, the interfered (orange) curve was very different, dropping at each SF boundary but steadily increasing the further away from a gateway. After consideration, it was noted how the two losses are treated independently in stochastic

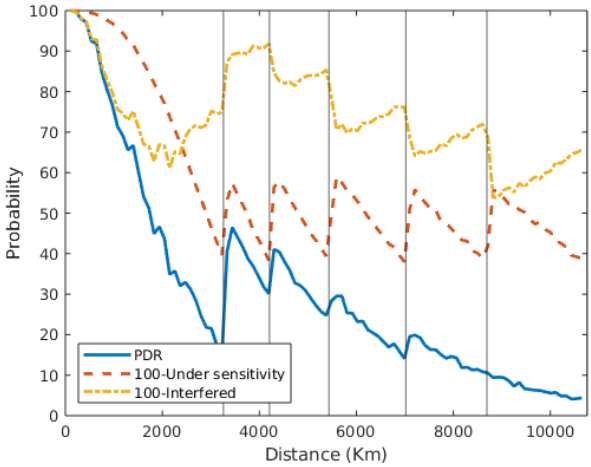


Fig. 3: Initial result for the PDR (blue) and the complementary to the outage probabilities as a function of a node's distance from a gateway

models and calculated regardless of one another. In reality and in the NS-3 simulation, this is not the case.

A packet needs first of all to be locked on by a gateway by having a high enough power, hence surviving the sensitivity check. Only then it can collide (fail because of interference with others). Therefore, while not all packets are checked for collision (in case they already failed the sensitivity check), their power always adds up to the interference on that SF.

While this discrepancy was not easily fixed because of the way the NS-3 simulator works, a good compromise was reached by simply acknowledging that the number of packets that collide is not a percentage of all packets sent but a percentage of the number of packets that have already successfully passed the sensitivity check. By modifying the plot accordingly, Fig. 4 is reached, which this time is very similar in all three curves.

The final small discrepancy is the performance at SF12. Despite the network is shown to perform roughly 5-10% better in simulation than in the model while using the highest possible SF, we believe this error is tolerable when comparing the two different methods. This is especially the case considering that some assumptions of the stochastic setup, such as the shorter ToA and the random time interval between packets were not perfectly replicable in NS-3.

## VI. Conclusion

Although both have their strengths and weaknesses, this study shows that stochastic geometry models and discrete-time simulations are equivalent tools when analysing the performance of a LoRaWAN network. This is provided that some key differences between the two methods regarding inter-dependency of aspects of the protocol behaviour are clearly understood and accounted for.

In future research, this same analysis will be carried out, but reverting the NS-3 LoRaWAN modules to perform as

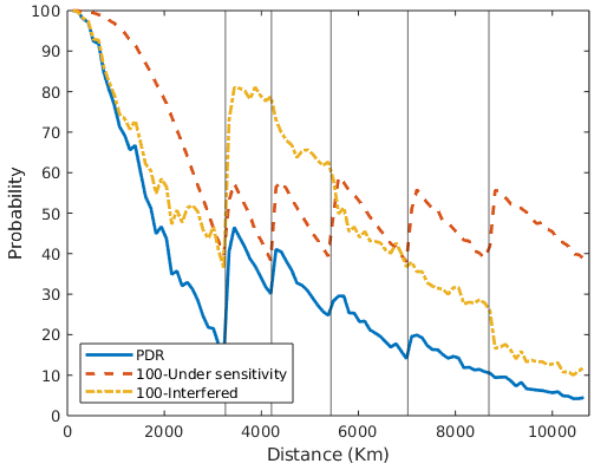


Fig. 4: PDR (blue) and complementary to the outage probabilities as a function of a node's distance from a gateway by taking into account timing discrepancies between the two analysis methods.

they would in a more realistic scenario, instead of matching the existing stochastic model results, which are generally operating under simplified behavioural assumptions.

## Acknowledgement

The authors would like to thank the UK EPSRC supporting Bruno Citoni PhD studentship through grant EP/R512266/1, and to acknowledge the support of the wider Communication Sensing and Imaging (CSI) research group, School of Engineering, University of Glasgow.

## References

[1] B. Citoni, F. Fioranelli, M. A. Imran, and Q. H. Abbasi, "Internet of things and lorawan-enabled future smart farming," *IEEE Internet of Things Magazine*, vol. 2, no. 4, pp. 14–19, 2019.

[2] P. Ferrari, E. Sisinni, D. F. Carvalho, A. Depari, G. Signoretti, M. Silva, I. Silva, and D. Silva, "On the use of lorawan for the internet of intelligent vehicles in smart city scenarios," in *2020 IEEE Sensors Applications Symposium (SAS)*, 2020, pp. 1–6.

[3] T. R. Wanasinghe, R. G. Gosine, L. A. James, G. K. I. Mann, O. de Silva, and P. J. Warrian, "The internet of things in the oil and gas industry: A systematic review," *IEEE Internet of Things Journal*, vol. 7, no. 9, pp. 8654–8673, 2020.

[4] A. Augustin, J. Yi, T. Clausen, and W. M. Townsley, "A study of Lora: Long range & low power networks for the internet of things," *Sensors (Switzerland)*, vol. 16, no. 9, 2016.

[5] R. Sanchez-Iborra and M. D. Cano, "State of the art in LP-WAN solutions for industrial IoT services," *Sensors (Switzerland)*, vol. 16, no. 5, 2016.

[6] F. Adelantado, X. Vilajosana, P. Tuset-Peiro, B. Martinez, J. Melia-Segui, and T. Watteyne, "Understanding the limits of lorawan," *IEEE Communications Magazine*, vol. 55, no. 9, pp. 34–40, Sep. 2017.

[7] O. Georgiou and U. Raza, "Low Power Wide Area Network Analysis: Can LoRa Scale?" *IEEE Wireless Communications Letters*, vol. 6, no. 2, pp. 162–165, 2017.

[8] F. Cuomo, M. Campo, A. Caponi, G. Bianchi, G. Rossini, and P. Pisani, "Explora: Extending the performance of lora by suitable spreading factor allocations," in *2017 IEEE 13th International Conference on Wireless and Mobile Computing, Networking and Communications (WiMob)*, Oct 2017, pp. 1–8.

[9] D. Magrin, M. Centenaro, and L. Vangelista, "Performance evaluation of LoRa networks in a smart city scenario," *IEEE International Conference on Communications*, 2017.

[10] M. Centenaro, L. Vangelista, A. Zanella, and M. Zorzi, "Long-range communications in unlicensed bands: the rising stars in the iot and smart city scenarios," *IEEE Wireless Communications*, vol. 23, no. 5, pp. 60–67, October 2016.

[11] D. Croce, M. Gucciardo, S. Mangione, G. Santaromita, and I. Tinnirello, "Impact of LoRa Imperfect Orthogonality: Analysis of Link-Level Performance," *IEEE Communications Letters*, vol. 22, no. 4, pp. 796–799, 2018.

[12] O. Georgiou, C. Psomas, C. Skouroumounis, and I. Krikidis, "Optimal Non-Uniform Deployments of LoRa Networks," *IEEE Wireless Communications Letters*, vol. 2337, no. c, pp. 1–1, 2020.

[13] O. Georgiou, C. Psomas, and I. Krikidis, "Coverage Scalability Analysis of Multi-Cell LoRa Networks," *IEEE International Conference on Communications*, vol. 2020-June, 2020.

[14] A. Mahmood, E. Sisinni, L. Guntupalli, R. Rondon, S. A. Hassan, and M. Gidlund, "Scalability Analysis of a LoRa Network under Imperfect Orthogonality," *IEEE Transactions on Industrial Informatics*, vol. 15, no. 3, pp. 1425–1436, 2019.

[15] R. B. Sørensen, N. Razmi, J. J. Nielsen, and P. Popovski, "Analysis of LoRaWAN Uplink with Multiple Demodulating Paths and Capture Effect," *IEEE International Conference on Communications*, vol. 2019-May, 2019.

[16] M. C. Bor, U. Roedig, T. Voigt, and J. M. Alonso, "Do lora low-power wide-area networks scale?" in *Proceedings of the 19th ACM International Conference on Modeling, Analysis and Simulation of Wireless and Mobile Systems*, ser. MSWiM '16. New York, NY, USA: ACM, 2016, pp. 59–67. [Online]. Available: http://doi.acm.org/10.1145/2988287.2989163

[17] E. Sallum, N. Pereira, M. Alves, and M. Santos, "Performance optimization on LoRa networks through assigning radio parameters," *Proceedings of the IEEE International Conference on Industrial Technology*, vol. 2020-February, pp. 304–309, 2020.

[18] Sugianto, R. Harwahyu, A. A. Anhar, and R. F. Sari, "Simulation of mobile LoRa gateway for smart electricity meter," *International Conference on Electrical Engineering, Computer Science and Informatics (EECSI)*, vol. 2018-October, pp. 292–297, 2018.

[19] F. Cuomo, J. C. C. Gamez, A. Maurizio, L. Scipione, M. Campo, A. Caponi, G. Bianchi, G. Rossini, and P. Pisani, "Towards traffic-oriented spreading factor allocations in LoRaWAN systems," *2018 17th Annual Mediterranean Ad Hoc Networking Workshop, Med-Hoc-Net 2018*, pp. 1–8, 2018.

[20] F. Cuomo, M. Campo, E. Bassetti, L. Cartella, F. Sole, and G. Bianchi, "Adaptive mitigation of the Air-Time pressure in LoRa multi-gateway architectures," *arXiv*, pp. 56–61, 2019.

[21] F. V. Abeele, J. Haxhibeqiri, I. Moerman, and J. Hoebeke, "Scalability analysis of large-scale LoRaWAN networks in ns-3," *arXiv*, vol. 4, no. 6, pp. 2186–2198, 2017.

[22] Y. Oukessou, M. Baslam, and M. Oukessou, "LPWANIEEE 802.11ah and LoRaWAN capacity simulation analysis comparison using NS-3," *Proceedings of the 2018 International Conference on Optimization and Applications, ICOA 2018*, pp. 1–4, 2018.

[23] J. Finnegan, S. Brown, and R. Farrell, "Modeling the Energy Consumption of LoRaWAN in ns-3 Based on Real World Measurements," *2018 Global Information Infrastructure and Networking Symposium, GIIS 2018*, pp. 0–3, 2019.

[24] D. Magrin, M. Capuzzo, A. Zanella, and M. Zorzi, "A Configurable Mathematical Model for Single-Gateway LoRaWAN Performance Analysis," 2019. [Online]. Available: http://arxiv.org/abs/1912.01285